

A CFD-model describing filtration, regeneration and deposit rearrangement effects in gas filter systems

Timo Deuschle^{a,*}, Uwe Janoske^{b,1}, Manfred Piesche^{a,2}

^a Institute of Mechanical Process Engineering, University of Stuttgart,
Boeblingen Straße 72, D-70199 Stuttgart, Germany

^b University of Cooperative Education, Lohrtalweg 10, D-74821 Mosbach, Germany

Received 15 August 2006; accepted 7 March 2007

Abstract

Due to ever increasing demands regarding filtration processes, filter development is faced with the task to understand these processes in a more detailed way. For this purpose, the computational fluid dynamics (CFD) is a helpful tool. This paper presents an experimentally validated CFD-model describing filtration, regeneration and deposit rearrangement effects in a gas filter system.

© 2007 Elsevier B.V. All rights reserved.

Keywords: Numerical simulation; Filtration; Regeneration; Deposit rearrangement; Gas filtration; Automotive; Exhaust aftertreatment; Diesel particulate filter

1. Introduction

Among separation processes, filtration has shown to be an effective method for removing particles from polluted fluid flows and is therefore applied in very different applications. A filtration process can be split up in three main characteristic steps. First, the particle filtration, which leads to a deposition of particulate matter in the filter, second the occasional regeneration of the filter system in case the gas filter system is not a single-use device and third, depending on the filtration and regeneration conditions, the rearrangement of the deposits collected on and in the filter influencing further filtration characteristics of the system.

A great challenge is the development of gas filter systems coping with the above-mentioned effects as they can be found in the reduction of environmentally harmful diesel exhaust particulate emissions of passenger cars. In order to meet legal emission standards, there exist demands to reduce the particulate content in the exhaust of diesel engines to a minimum. Today, aftertreatment devices, such as a diesel particulate filter (DPF) are used. Most of the DPF systems that are used nowadays work on similar

principles. The emitted particles, mainly carbon soot particles, are collected on and in a filter with a large surface area. The DPF consist either of porous ceramic or of sintered metal having to stand the high temperatures of the exhaust. Due to the particle loading of the filter, the exhaust gas back pressure over the DPF increases together with the fuel consumption of the car. To work against this increase, the DPF gets regenerated from time to time by incinerating the collected particles. However, the exhaust temperature of a passenger car under normal operating conditions is not high enough to ignite the soot particles. For this reason, the combustion of the accumulated soot in the DPF must be specifically induced in regular intervals in order to regenerate the DPF. Thus, to facilitate the regeneration of the DPF, systems with catalytic additives in the fuel or catalyst-coated DPF are applied to lower the necessary regeneration temperature. Apart from the burnable soot particles there is an amount of particles collected in the DPF that consists of metal oxides and sulfates therefore being not combustible within the thermal regeneration. These inert deposits form a permanent ash layer, which partially locks the effective filtration area of the DPF in the long run and shortens the life-time of the device. With further operation time, these ash deposits might get rearranged inside the DPF depending on the loading and the regeneration conditions and therefore influence the dynamic characteristic of the device, e.g. regarding the pressure drop.

In this paper, an experimentally validated CFD-model is presented describing the filtration and the regeneration effects in a

* Corresponding author. Tel.: +49 711 641 2209; fax: +49 711 641 2390.

E-mail address: deuschle@imvt.uni-stuttgart.de (T. Deuschle).

¹ Tel.: +49 6261 939 478; fax: +49 6261 939 544.

² Tel.: +49 711 641 2209; fax: +49 711 641 2390.

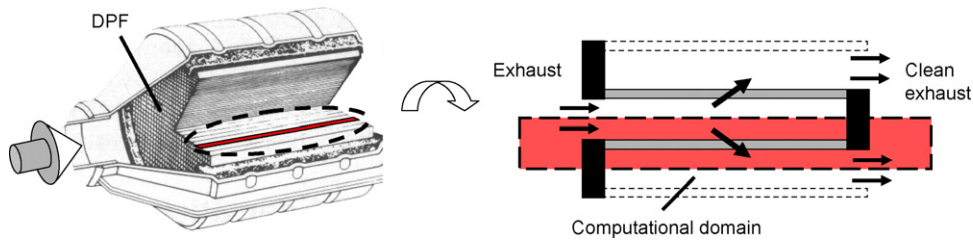


Fig. 1. DPF geometry and 2D computational domain.

gas filter system including the above-mentioned formation and rearrangement of incombustible deposits. A diesel particulate filter is considered as an example.

2. Model development

Standard CFD-codes do not have the ability to calculate the above-described dynamic filtration and regeneration processes in gas filter systems. For this reason a commercial CFD-code (FLUENT 4™) is expanded with self-developed program routines written with FORTRAN programming language that are coupled to the CFD-code through defined user interfaces. In the following section the basics of a simulation model regarding a diesel particulate filter are explained and a description of the coupled simulation procedure is given.

2.1. Geometry and calculation area

In this study a silicon carbide wall-flow DPF is investigated. A wall-flow DPF consists of alternating open and closed filter channels. The exhaust is thereby forced to pass through a ceramic wall inside the DPF separating the solid particles from the fluid flow. The DPF is implemented in the exhaust system of passenger cars. A DPF geometry with a cut-out illustrating the used 2D computational domain can be seen in Fig. 1.

In order to minimize the computational effort for the calculations, the loading, regeneration, and rearrangement effects in the DPF are only examined in a single inlet/outlet channel pair of the DPF. Preliminary numerical investigations with a three-dimensional model showed a uniform flow distribution over the main part of the inlet cross-section of a circular wall-flow DPF [1,2]. Thus, the reduction of the simulation model to two dimensions is a valid assumption. The flow inside the channels is assumed to be symmetric, therefore only half of the

inlet and half of the outlet channel have to be considered in the computational domain. This means, the effects of loading, regeneration and deposit rearrangement are determined for a single filter wall inside the DPF. The computational domain also includes the incoming and outgoing flow and is thereby able to represent contraction and expansion of the flow. The computational grid is composed of rectangular elements. Particular attention is given to the soot layer and the ceramic wall to reach a high resolution of the separation process. In Fig. 2 a cut-out of the computational grid, focusing on the surface layer and the ceramic wall, is shown enlarged.

The height of the control volumes (CV) of the surface layer is dynamically adapted according to the DPF deposit loading, contrary to the height of the CV in the ceramic, which remain constant. Thereby, the impact of the deposits on the flow field in the inlet channel is considered. This grid adaption has been discussed in greater detail in an earlier publication [3].

2.2. Simulation procedure

As described above, the CFD-code has to be coupled with self-developed program routines known as user defined sub-routines (UDS) for describing the dynamic effects of filtration, regeneration and deposit rearrangement. An overview of the iterative simulation procedure is given in Fig. 3.

After the definition of the gas filter geometry and the computational domain, the fluid flow and the particle tracks of the exhaust emissions are computed using the commercial CFD-code. Thereby, the fluid flow is calculated by solving the continuity and the Navier–Stokes equations. The particle tracks of the solid exhaust emissions are determined using an Euler–Lagrange approach where the particles are regarded as mass points. The particle trajectories are computed by integrating the forces acting on each particle until the particle impinges on the pre-defined filter media, in case of the DPF, the ceramic

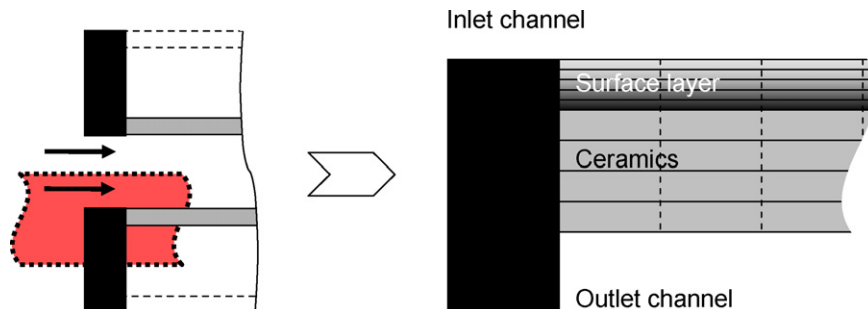


Fig. 2. Computational grid in the vicinity of the surface layer and the ceramics.

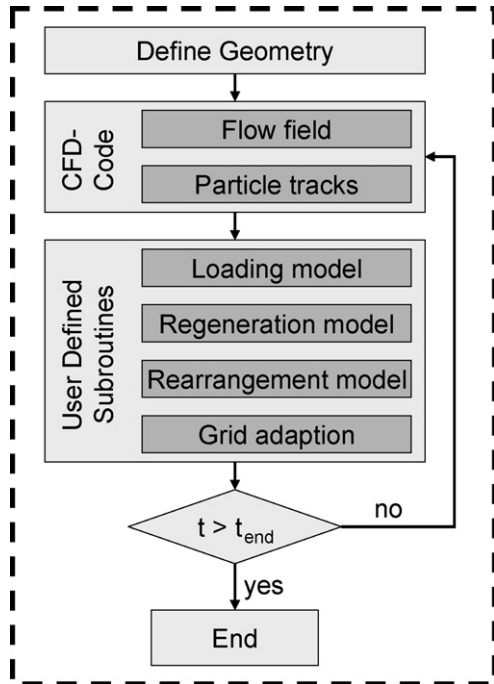


Fig. 3. Simulation procedure.

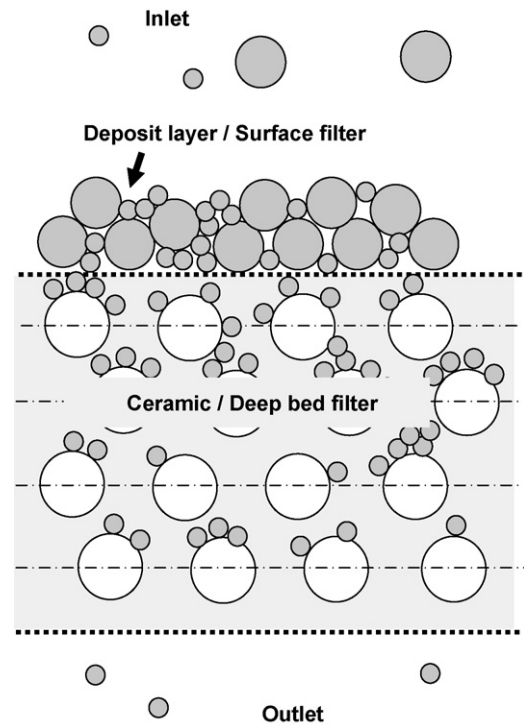


Fig. 4. Filtration mechanism.

wall. It has to be noted that the CFD-model is able to work with real particle size distributions, e.g. measured at an engine test bench, and handles up to five different particle species (e.g. soot, unburned hydrocarbons, metal oxides).

In order to ensure acceptable computation times the following assumptions were made for the simulation:

- fluid has Newtonian behavior;
- quasi-steady, laminar flow;
- particles are spherical;
- homogeneous distribution of particles over the inlet area;
- low concentration of solid particles in the fluid;
- no particle–particle interaction;
- no particle–fluid interaction (one-way coupling).

The results of the flow field and particle track calculation are the input information for the UDS. Based on the particle impinging locations on the ceramic wall, in the next simulation step the separated particles on and in the ceramics material are determined with the “Loading model” that is based on a modified fiber separation model [4], where a differentiation between a surface filtration and a deep bed filtration is included (Fig. 4).

The separated particle mass stream (\dot{m}_{sep}) can be determined with the calculated over-all separation efficiency (θ_{all}) in each CV:

$$\dot{m}_{\text{sep}} = \dot{m}[1 - e^{(-k_f\theta_{\text{all}})}] \quad (1)$$

A more detailed description of the separation mechanism and the mass deposition including the determination of the over-all separation efficiency θ_{all} and the material constant k_f is given elsewhere [5]. The deposits lead to a locally increased flow resistance and the resulting pressure drop over the deposit layer

and the ceramics is calculated in each CV using an adapted Carman–Kozeny relation [4]:

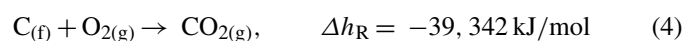
$$\Delta p = k \frac{(1 - \varepsilon)^2}{\varepsilon^3} v \mu \frac{h}{d^2} \quad (2)$$

Here, k is a material constant, ε the porosity, v the velocity normal to the filter media, μ the dynamic viscosity, h the height of the CV and d is the mean particle diameter of the deposited particles for either a CV in the deposit layer or in the ceramics material. For a new calculation of the flow field, the pressure loss is considered in the momentum equation through sink terms.

The subsequent regeneration step considers a temperature-induced regeneration of the DPF and evaluates the development of the deposits in the surface layer and in the depth of the ceramics with time. The basis of the “Regeneration model” is the solution of the energy balance [6] for all materials considered (ceramics, soot, ash) in each CV of the surface layer and the ceramics:

$$\begin{aligned} \frac{\partial T}{\partial t} + \varepsilon \rho c_p \left(u \frac{\partial T}{\partial x} + v \frac{\partial T}{\partial y} \right) \\ = \lambda_{\text{eff}} \left(\frac{\partial^2 T}{\partial x^2} + \frac{\partial^2 T}{\partial y^2} \right) + \dot{q}_{\text{Diss}} + \text{ST} \end{aligned} \quad (3)$$

Through the source term ST the exothermal energy release of the chemical reaction of the soot oxidation is implemented in the energy balance. Within the “Regeneration model” the soot oxidation is modelled as a complete combustion of carbon:



Thus, at increased temperatures the reaction is leading to a decrease of the deposited soot mass $m(t)$. Furthermore, the reaction is leading to an increase of the inert ash mass m_{Ash} , e.g. if catalytic additives are used:

$$\frac{dm}{dt} = -m(t)RR \quad (5)$$

$$\frac{dm_{\text{Ash}}}{dt} = -F \frac{dm}{dt} \quad (6)$$

The increase of the mass of ash depends on the underlying type of regeneration. A thermal regeneration (based on oxygen) leads to less mass of ash in comparison to a continuous regeneration (based on nitrogen dioxide). The parameter F has been gained from experimental results [3]. Next to the deposit decrease and increase, the temperature distribution caused by the exothermal reaction in the filter media is determined. Therefore, the reaction rate RR of the oxidation (Eq. (4)) is described as a product of the number of active sites N on the surface of the filter media and the function for the temperature dependency $k(T)$ of the reaction rate [7]:

$$RR = N(\xi)k(T) \quad (7)$$

The number of active sites N is a function of the conversion rate ξ . In the “Regeneration model” an approach from Bhatia–Perlmutter [8] is implemented to consider the change of the reaction surface. The temperature dependency of the reaction rate is described by an Arrhenius law including the frequency factor k_0 and the activation energy E :

$$k(T) = k_0 e^{(-E/RT)} \quad (8)$$

With this data the source term ST in the energy balance can be determined. ST is a function of the reaction rate RR , of the net calorific value of the soot H_u and of the deposited soot mass $m(t)$ [6]:

$$ST = f(RR, H_u, m(t)) \quad (9)$$

Finally, by solving the energy balance using an explicit solution method, the temperature field is determined in each CV of the surface layer and in the depth of the ceramics.

The type of regeneration (thermal or continuous) also defines the behavior of the ash layer with ongoing operation of the DPF [3] and is considered within the “Rearrangement model”. Within the “Rearrangement model” there is a differentiation between ash forming out crusty deposit layers along the ceramic wall of the DPF (from continuous regeneration) and ash getting rearranged inside the DPF inlet channels (from thermal regenerations). Experimental data gained at an engine test bench and a subsequent analysis of the depositions in the DPF using computer tomography (CT) showed these different ash depositions [3] as they can be seen in Figs. 5 and 6.

For that reason, in the “Rearrangement model” for ash from a thermal regeneration a rearrangement of the deposits towards the end of the DPF inlet channel is considered in contrary to ash from a continuous regeneration blocking the ceramic wall surface over the complete channel length. The behavior of the ash

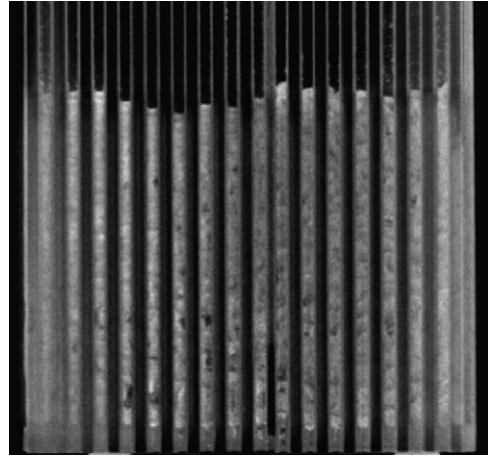


Fig. 5. Computer tomography (CT) picture, cross-section of a DPF with depositions after a thermal regeneration.

layer strongly influences the permanent increase of the pressure drop over the DPF device as it can be seen in Section 3.

With the results gained from the computation of the three sub-models the locations of the deposits along the DPF channel are known and in the following step a grid adaption is performed such that the grid matches the surface layer topology. The procedure described above is repeated until a pre-defined simulation time is reached. Within a single quasi-steady time step containing either loading, regeneration or rearrangement effects a constant flow field is assumed. The transient filtration and regeneration process caused by an increase and decrease of the deposit height and changing operating conditions is described with a quasi-steady approach.

A main benefit of the described CFD-model is the modular structure containing the different UDS allowing a very flexible control of the simulation procedure. With the CFD-model, it is possible to compute any defined operation cycle of a gas filter system including defined loading and regeneration operating conditions, driven for example at an engine test bench.

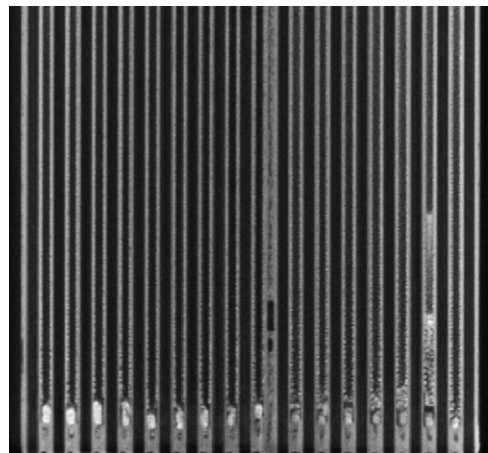


Fig. 6. Computer tomography (CT) picture, cross-section of a DPF with depositions after a continuous regeneration.

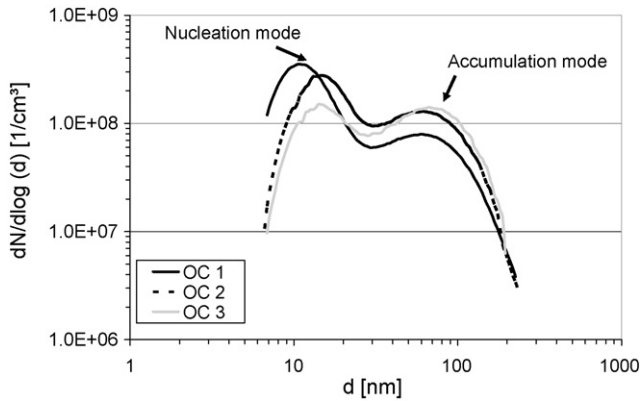


Fig. 7. Particle size distribution of the exhaust.

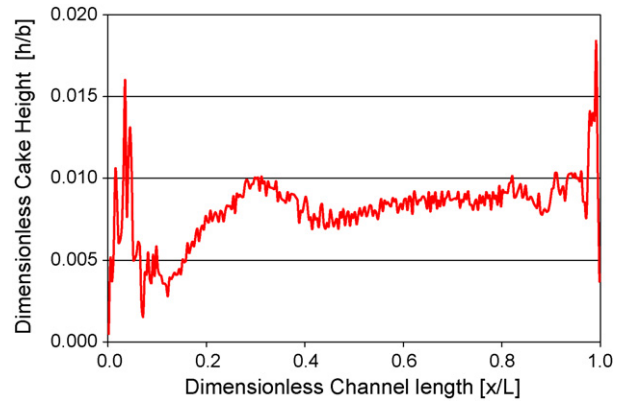


Fig. 9. Surface layer topology vs. channel length.

3. Results

The experimental validation of the simulation model was performed on an engine test bench [3]. The engine used was a DaimlerChrysler 2.7l with a common rail direct injection. The exhaust track was equipped with an upstream series oxidation catalyst and a consecutive DPF (5.66 in. \times 6 in., 180/16). An important matter regarding any gas filtration process and its specific separation efficiency is the particle size distribution of the gas flow to be cleaned. The number particle size distributions in pre-defined engine operating conditions (OC) are given in Fig. 7.

For the computation of the particle tracks within the CFD-model a representative particle size distribution consisting of eight particle classes for the pre-defined OC was used. At the engine test bench the pressure drop over the DPF as a function of time is recorded. A pressure drop graph can be seen in Fig. 8 for three consecutive OC together with the computational results of the simulation model.

It is evident that the CFD-model is capable of accurately determining the behavior of the pressure drop over the DPF with increasing time and soot loading including a change of the OC defined by revolutions per minute and torque.

Furthermore, the CFD-model offers detailed data on the transient behavior of the surface layer. In Fig. 9 a graph of the

dimensionless surface layer topology as a function of the dimensionless inlet channel length is given, where b is the channel width and L the channel length. By evaluating this result the dominating deposition locations can be detected.

For validating the regeneration process of the DPF, the device is loaded definitely at the engine test bench and is thereafter regenerated at a pre-defined OC. By using pre-defined OC a comparison of different specific loading and regeneration conditions of the DPF is possible. One result of a DPF regeneration comparing simulation and experiment is given in Fig. 10.

During the DPF regeneration the pressure drop declines noticeably caused by the ignited soot combustion. In order to confirm the efficiency of the regeneration, the DPF is afterwards partially loaded at the same OC used before. The DPF regeneration shown in Fig. 10 has a very high efficiency, thus bringing the value of the pressure drop down to the initial one before loading the DPF. The increase of the pressure drop at the start of the regeneration is caused by the elevated temperatures inside the DPF through the exothermal reaction. For the loading and regeneration conditions investigated, the simulation model is able to correctly determine the change of the pressure drop over the DPF after regeneration including the pressure drop increase at the beginning of the regeneration. Further investigations of the results of the CFD-model with partial regenerated DPF have

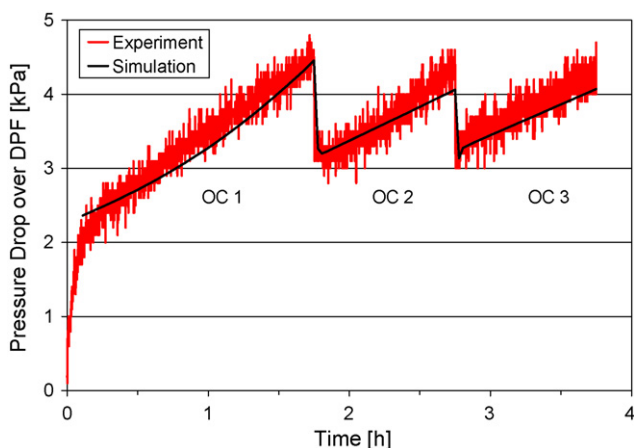


Fig. 8. DPF loading, pressure drop vs. time.

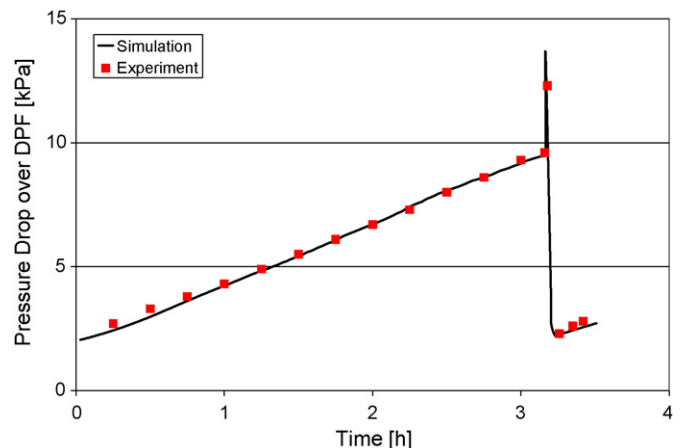


Fig. 10. DPF loading/regeneration, pressure drop vs. time.

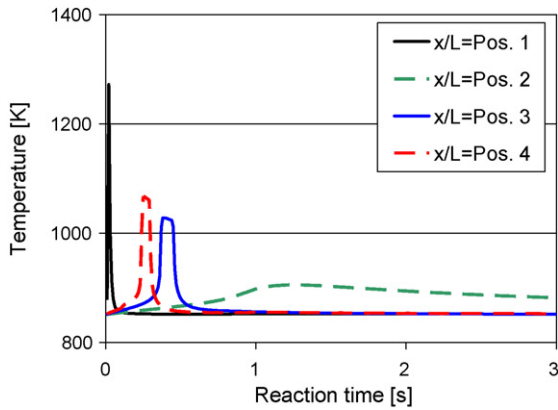


Fig. 11. Temperature distribution in the surface layer.

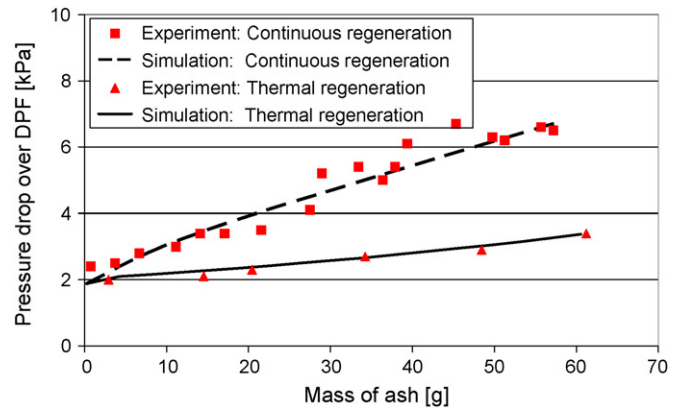


Fig. 12. Ash rearrangement, pressure drop vs. time.

also shown a very good agreement. An additional result of the regeneration sub-model is the two-dimensional temperature distribution over the surface layer and the ceramics. In Fig. 11 a temperature development in the surface layer is given for different locations along the channel length as a function of the reaction time. With this detailed temperature information it is possible to detect critical areas of high temperature inside of the DPF and “worst-case” scenarios can be computed, representing extreme situations of the DPF, e.g. a highly soot loaded DPF being regenerated with the fluid flow through the device being not high enough to sufficiently “cool” down the DPF.

To validate the influence of the dynamic deposit rearrangement inside the DPF, long-term runs were performed at the engine test bench consisting of numerous DPF loadings and regenerations. With each regeneration, the accumulated mass of ash increases and therefore the effect of the ash accumulation on the pressure drop over the DPF can be reported. From these experimental investigations at the engine test bench together with subsequent computer tomography analyses of the DPF [6] it is known that there is a difference between ash from a thermal regeneration and ash from a continuous regeneration (see Figs. 5 and 6). To investigate this difference in detail, experiments were performed at the engine test bench recording the pressure drop with increasing mass of ash at a constant measuring OC. For the thermal regeneration the pressure drop was measured and compared always directly after each regeneration cycle. For the continuous regeneration the measuring OC was briefly driven on the engine test bench from time to time before returning to the specific OC with defined continuous regeneration. Using the same measuring OC, the results regarding the pressure drop can be compared directly, as it can be seen in Fig. 12. There the computational results of the simulation model are also shown.

Regarding the same accumulated mass of ash, the “continuous ash” formed out as a crusty layer leads to a larger increase of the pressure drop over the DPF than the “thermal ash” depositions at the end of the inlet channel. In both cases the simulation results agree very well with the data gained from the engine test bench. The described experimental investigations validate the CFD-model and prove its capability of simulating engine test bench cycles consisting of a multitude of DPF loading OC and

cyclic regenerations including the important increase in back pressure caused by the formation of regeneration-specific ash depositions inside the DPF.

4. Conclusions

Within this work a CFD-model was developed that describes the filtration, the regeneration and the deposit rearrangement effects in a gas filter system. The simulation model is presented using a diesel particulate filter as an exemplary gas filter system of high interest in the automotive engineering area. The model was validated through experimental results gained from an engine test bench coupled with detailed analyses of the deposits in the DPF using computer tomography. The CFD-model was shown to be capable of simulating engine test bench cycles including DPF loading and cyclic combustion of the deposits at varying operating conditions with the consideration of the irreversible increase in exhaust gas back pressure caused by the formation of a regeneration-specific ash layer inside the DPF. Altogether the CFD-model serves to investigate the long-term behavior of a gas filter system, e.g. a diesel particulate filter, with respect to the permanent increase in back pressure caused by inert depositions accumulated inside the filter system with persisting operation time. Complex and time consuming experimental investigations, such as those found in the gas filter system development could be substantially reduced through the use of this simulation model. The impacts of changes in important influencing quantities regarding filter loading and regeneration, e.g. particle concentration or mass flow, can quickly be examined and studied in detail. These results can then be used for the design and development of new gas filter systems.

In addition, the simulation model could also be applied to other gas filter system geometries. In the special case of a DPF wall-flow filter geometry, for instance with different channel widths, ceramic wall thicknesses, channel lengths or different ratios of inlet-to-outlet cross-sectional areas. Filter channels with cross-sectional areas that change over the length of the filter can also be investigated. Furthermore, the simulation model can be extended to simulate catalyst-coated gas filter systems optimizing the filter regeneration. Finally, due to the modular setup

of the simulation model further sub-models can be implemented, for example to consider aging effects of the depositions.

Acknowledgement

The authors gratefully acknowledge the financial support and useful contributions to this work from the “Forschungsvereinigung Verbrennungskraftmaschinen e. V. (FVV e.V.)”.

References

- [1] E.J. Bissett, Mathematical model of the thermal regeneration of a wall-flow monolith diesel particulate filter, *Chem. Eng. Sci.* 39 (7/8) (1984) 1233–1244.
- [2] A.G. Konstandopoulos, J.H. Johnson, Wall-flow diesel particulate filters—their pressure drop and collection efficiency, *SAE Technical Paper Series*, 890405, 1989.
- [3] M. Piesche, M. Bargende, T. Deuschle, G. Hitzler, Langzeitstabilität von Partikelfiltern in Dieselmotoren, FVV-Forschungsvorhaben, Abschlussbericht, Heft 805, 2005.
- [4] F. Löffler, Staubabscheiden Lehrbuchreihe Chemieingenieurwesen/Verfahrenstechnik, Georg Thieme Verlag, 1988.
- [5] C.N. Opris, J.H. Johnson, A 2D computational model describing the flow and filtration characteristics of a ceramic particulate trap, *SAE Technical Paper Series* 980545, 1998.
- [6] C.N. Opris, J.H. Johnson, A 2D computational model describing the heat transfer, reaction kinetics and regeneration characteristics of a ceramic particulate trap, *SAE Technical Paper Series* 980546, 1998.
- [7] J.P.A. Neeft, et al., Kinetics of the oxidation of diesel soot, *Fuel* 76 (12) (1997) 1129–1136.
- [8] S.K. Bhatia, D.D. Perlmutter, A Random pore model for fluid–solid reactions. I. Isothermal, kinetic control, *AIChE J.* 26 (3) (1980) 379–386.